The dosimetric impact of intra- and interfractional motion of lungs and kidneys for total body irradiation delivered with volumetric modulated arc therapy

Author: H.Y. Buiting

Date: 18-12-2024

TU Delft

The dosimetric impact of intra- and interfractional motion of lungs and kidneys for total body irradiation delivered with volumetric modulated arc therapy

By

H.Y. Buiting

In partial fulfilment of the requirements for the degree of:

Master of Science
in Biomedical Engineering

at the Delft University of Technology,
to be defended publicly on Wednesday December 18, 2024 at 9:30 AM.

Supervisor:	M.C. Goorden PhD	
	E. Seravalli PhD	
Thesis committee:	M.C. Goorden PhD,	TU Delft
	R.M. de Kruijff PhD,	TU Delft
	E. Seravalli PhD,	UMC Utrecht

The dosimetric impact of intra- and interfractional motion of lungs and kidneys for total body irradiation delivered with volumetric modulated arc therapy

Hidde Yannick Buiting BSc

***Abstract*—Purpose: Organ motion may have an impact on the radiation dose administered in radiotherapy. Motion can occur during treatment (intrafractional motion) or between fractions of treatment (interfractional motion). A clinically relevant dosimetric impact on OAR would mean that additional measures such as 4D-CT planning or a PRV are needed. In this study, the dosimetric impact of intra- and interfractional motion is studied for TBI delivered with VMAT is studied.**

Method: For the intrafractional part, motion magnitude was determined with 4D-CT data, and this magnitude was used to expand and reduce the volumes of the OAR in 27 VMAT-TBI plans, dose was analyzed in these volumes. For the interfractional part, the CBCT images taken right before treatment are registered with the planning CT. The planning CT is then deformed to match the anatomy of the CBCT for each fraction. The dose is recalculated on this deformed CT and the mean dose in OAR volumes is evaluated for each fraction.

Results: For the intrafractional part, on average, an expansion with a typical respiratory motion magnitude results in a 0.3 Gy higher mean dose in the kidneys. This expansion results in a 0.6 Gy higher mean dose in the left lung and a 0.8 Gy higher dose in the right lung. For the interfractional part, the mean dose difference between the fraction with the lowest mean dose and the one with the highest mean dose was 0.04 Gy on average.

Conclusion: After discussing these dose differences with a radio-oncologist, it was concluded that these differences were not clinically relevant. Therefore, 4D-CT planning and a PRV are not necessary.

***Index Terms*—Radiotherapy, VMAT, TBI, respiratory motion, organs at risk.**

I. Introduction

EXTERNAL beam radiotherapy is used for non-invasive treatment of various types of cancer. Radiation dose is delivered to the patient with the aim of destroying cancer cells, often divided into multiple fractions. In this process, radiation dose is delivered to a predefined target volume and to healthy tissue as well. A healthy organ near the target volume that can be damaged by radiation during treatment is termed an organ at risk (OAR). This dose distribution is planned on a computed tomography (CT) image acquired with the patient in treatment position. In treatment planning, the target and OAR volumes are defined and margins may be used around these volumes to account for geometrical uncertainties. A planning target volume (PTV) is used to account for these uncertainties and to deliver the prescribed dose in the target volume. A planning organ at risk volume (PRV) can be used to account for these uncertainties when the OAR dose must be below a certain constraint [1]. This treatment planning can be performed on a 3D-CT or on a 4D CT. 3D-CT is a medical imaging procedure that uses computer-processed reconstruction of many projections from different angles to produce cross-sectional images of a sample [2]. 4D-CT is a similar imaging procedure that creates 3D-CT images at different phases over a single respiratory cycle. 4D-CT can be used in treatment planning by expanding PTV or PRV with a depicted extent of motion. An alternative use for 4D CT is to use tracking systems or gating methods to increase the likelihood of treating during a specific respiratory phase [3]. This CT scan is central in radiotherapy treatment planning because CT images contain electron density information that is essential for dose calculation with heterogeneity corrections. In addition, CT images are geometrically robust, which is essential for accurate tumor targeting during treatment planning and treatment delivery [4]. Conformal radiotherapy techniques shape the radiation beam to closely fit the target and minimize the dose to the healthy tissue surrounding the target [5]. The precision of this treatment plan can be influenced by changes in the anatomy of the patient between planning and treatment delivery. These changes in patient anatomy are generally caused by swelling, changes in weight, or organ movement [6]. Organ motion can occur due to physiological processes such as cardiac motion, digestion, and respiratory motion. Motion during the fraction is referred to as intrafractional motion, and motion between fractions is referred to as interfractional motion.

A. Radiotherapy for total body irradiation

Total body irradiation (TBI) is a component of conditioning regimens used to prepare leukemia patients for hematopoietic stem cell transplantation. It suppresses the immune system to prevent rejection of the graft and has the purpose of destroying malignant cells that have survived chemotherapy [6, 7]. Radiation is directed at the entire body. In TBI treatment, there are OARs in which a lower dose has to be considered. The radiation dose in the lens, lungs, and kidneys is bound to dose constraints to prevent treatment-induced organ dysfunction. The radiation dose in the lungs can induce pneumonitis, which can be life-threatening [7]. The radiation dose in the kidneys can induce chronic renal disease, which can require a kidney transplant or dialysis [8]. In TBI, the goal is to keep the mean

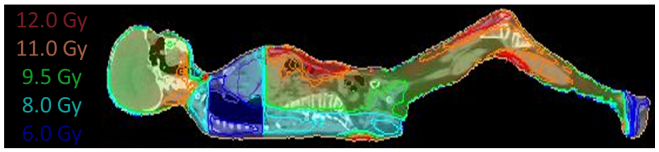

(a) Conventional TBI

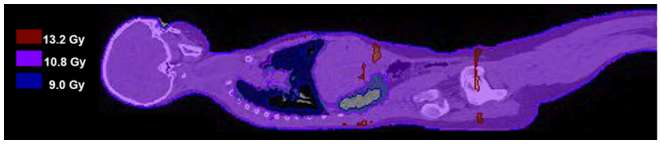

(b) VMAT-TBI

Fig. 1. Total body irradiation can be delivered with multiple methods. Image (a) shows a dose distribution in the sagittal plane that is typical for a conventional 2D radiotherapy delivery in combination with shielding. Image (b) shows a dose distribution in the sagittal plane that is typical for TBI with VMAT.

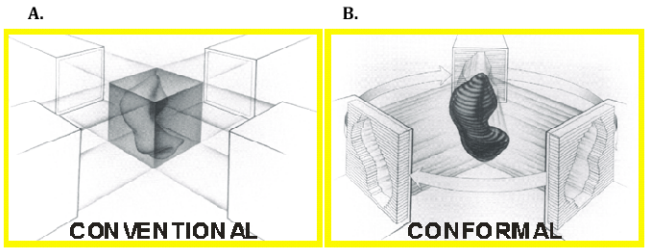

Fig. 2. A visual representation of both the conventional technique and the conformal technique. They gray volume represents the dose that is delivered by the beam. Conventional techniques use a uniform field and irradiate from two angles. VMAT is a conformal technique that delivers dose in a whole arc around the patient, and the shape and intensity is adjusted to closely fit the target [15].

dose in the kidneys below 10 Gy to prevent such side effects. Studies have suggested keeping the mean dose in the lungs below 8 Gy, but some institutes use a 10 Gy mean dose constraint. The goal is to keep the mean dose in the lens below 12 Gy, as a higher dose can lead to a cataract that needs surgery. These dose constraints are different across institutes [9]. These dose constraints are not hard, meaning that a higher dose may be administered in certain cases when keeping the dose below the constraint is infeasible. The rest of the body is the target volume where 12 Gy is prescribed.

In conventional TBI, shielding techniques are used in combination with 2D beam techniques to reduce radiation dose in the organs at risk [10]. In 2D beam techniques, parallel opposing beams are aimed at the patient perpendicular to the sagittal plane or coronal plane, depending on the center [11]. Institutes may use institute-developed chairs or beds that can put the patient in the treatment position, this can be an uncomfortable. This method in combination with shielding not only reduces the radiation dose in the organs at risk, but also reduces the dose in some bone marrow compartments [12]. The bone marrow compartments are an important part of the target volume, since hematopoietic stem cells are located in the bone marrow. Another disadvantage of conventional TBI is the inhomogeneous dose distribution, mainly due to tissue inhomogeneities, the contour of the body, and the beam energy [13]. Conventional TBI can deliver a dose below 80% or above 120% of the prescribed dose in the target volume, while the goal defined by the American Association of Physicists in Medicine is to stay within 90% and 110% of the prescribed dose [14]. In addition, calculations are often done manually instead of using a treatment planning system, and there is no precise reporting of the dose to the target or OAR. An example of a dose distribution in conventional TBI is shown in Figure 1a.

Conformal radiotherapy techniques are able to overcome these disadvantages. The dose can be delivered in a more homogeneous way, it can be planned, and patient positioning can be done on the treatment couch, which can be more comfortable. In addition, conformal techniques can spare organs at risk in a reliable way and still deliver sufficient dose in the surrounding target volume [5]. Using volumetric modulated arc therapy (VMAT) delivery for TBI, one can increase both conformality and homogeneity in target-dose distribution. VMAT consists of treating the patient by means of one or more gantry arcs with continuously varying beam aperture, gantry speed and dose rate. With this approach, patients can be treated with highly conformal dose distributions delivered with superior dosimetric accuracy in a time efficient way [16], an example of how this is done is shown in Figure 2. An example of a dose distribution of VMAT-TBI is shown in Figure 1b. Because of these advantages, some institutes use VMAT for TBI. In the UMC Utrecht, patients receive 12 Gy in 6 fractions of 2 Gy each delivered with VMAT with 6 MV beams. Patients are immobilized with a vacuum mattress and a mask. Due to the limited field size, the entire target volume may not be irradiated when the beam rotates around one point, such a point is called an isocenter. Depending on the height of the patient, four to seven isocenters are used in order to deliver dose in the entire target volume. A rotatable tabletop allowed rotation from head first to feet first orientation while the patient remained immobilized. Depending on the height of the patient, a rotation may be necessary. On average, treatment takes 43 minutes. Some aspects of this technique are still under evaluation. Currently, treatment planning is done on a 3D-CT, this is referred to as the planning CT. The planning CT is made before the series of radiotherapy fractions. In this type of imaging, motion is not measured because it does not take time into account. Therefore it does not account for intrafractional motion and the impact on radiation dose of this motion in organs at risk is unknown. A phantom study was conducted by Kavak *et al.* [6] to evaluate the dosimetric impact of intrafractional motion on dose in total marrow irradiation (TMI) delivered with VMAT. No study on dosimetric impact of intrafractional motion for TBI using real patient plans has been conducted yet. In addition, the effect of interfractional motion on radiation dose in the organs at risk is unknown for VMAT-TBI. In the UMC Utrecht, a cone beam computed tomography (CBCT) is made right before treatment. This is done with a CBCT scanner that is mounted on the linear accelerator and allows for position verification. With one single rotation, a volume can be imaged

TABLE I
AN OVERVIEW OF THE CHARACTERISTICS OF THE PATIENT POPULATION USED FOR THE MOTION ANALYSIS AND THE DOSIMETRIC STUDIES. THE NUMBER OF FRACTIONS THAT IS SHOWN IN THE INTERFRACTIONAL PART IS THE NUMBER OF FRACTIONS INCLUDED FOR THIS STUDY. ALL PATIENTS WERE TREATED IN SIX FRACTIONS. ANALYSIS ON THE KIDNEYS WERE DONE FOR THE LEFT (L) AND RIGHT (R) SIDE SEPARATELY.

Population characteristics	**Age (years)**	
	Average	**Range**
Surrogate patients	16	10-23
VMAT-TBI patients	15	5-32
Intrafractional study	**Organ**	
	Kidney	**Lung**
Surrogate patients	L: 20, R: 21	31
VMAT-TBI patients	26	27
Interfractional study	**Organ**	
	Kidney	**Lung**
Patients	L: 15, R: 14	22
Fractions	L: 89, R: 83	128

with a CBCT. However, these images are noisier than fan beam CT (FBCT) images such as the planning CT [17]. FBCT uses a row of detectors and a fan shaped beam, whereas CBCT uses a cone shaped beam and a flat panel detector. Since there are more photons at the same time, the cone shaped beam leads to more generated scatter than a fan shaped beam, and the flat panel detector measures more scattered photons than a row of detectors. Therefore, CBCT images are noisier than FBCT images. In addition, the accuracy of the assigned Hounsfield Unit (HU) is reduced in CBCT. Accurate HU assignment is central in radiotherapy planning in order to predict the radiation interaction with tissue and therefore the dose delivery. Due to these disadvantages, radiotherapy planning is done with FBCT. To present a treatment plan that is able to spare the organs at risk in a reliable way, the impact of organ motion on radiation dose needs to be studied. In this study, the impact of these two types of motion on the dose distribution for VMAT-TBI is investigated. A clinically significant impact of interfractional motion could lead to the need for a PRV, and a clinically relevant impact of intrafractional motion could lead to the need for a 4D-CT.

II. METHOD

A. Patient population

A retrospective study was conducted on 27 patients with an average age of 15, ranging from 5 to 32 years, who all underwent TBI with VMAT at the UMC Utrecht. In this group, the dosimetric impact of intrafractional and interfractional motion was studied. To study the effect of intrafractional motion, the motion magnitude of the lungs and kidneys had to be determined. 4D-CT data were used to determine the motion magnitudes. Since there are no available 4D-CT data on VMAT-TBI patients, 4D-CT data were used of patients of a similar age as TBI patients. This group of surrogate patients consisted of forty patients with an average age of 16 ranging from 10 to 23 years, all of whom received a 4D-CT at UMC Utrecht. The characteristics of the patient population are shown in Table I.

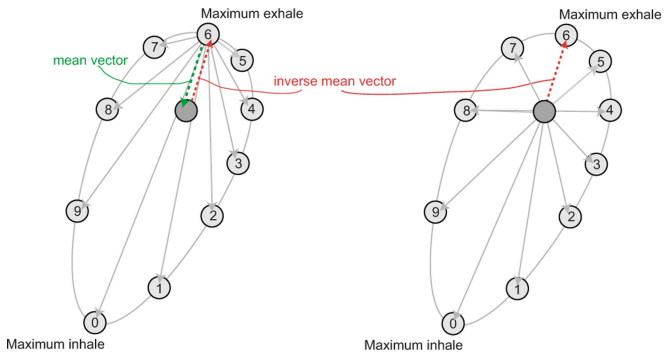

Fig. 3. A 2D representation of the midposition model. The respiratory phases determine a location of an individual voxel. A time weighted average for this voxel is calculated as well as the motion standard deviation in all directions [18].

B. Determining intrafractional motion magnitude

The group of surrogate patients was studied to find values for motion amplitudes. This was done for the kidneys, lungs, and ribcage for the left and right sides separately. Data were used from 20 surrogate patients for the left kidney and 21 patients for the right kidney. Some patients missed a kidney or, in some cases, either one was not well imaged on the 4D-CT. Data from 31 pairs of lungs and ribcages were analyzed. Only patients with two functional lungs were used in the analysis. Each 4D-CT data set consisted of ten phases. A time-weighted average of these ten phases was reconstructed using a midposition algorithm [18], shown in Figure 3. In addition to this time-weighted average image, images with motion data were computed. Data sets were generated with standard deviations of the motion in the left-right, anterior-posterior, and cranial-caudal axes. These sets with motion data provided information on volumes of interest; these volumes were manually delineated. The clinical delineations were used to analyze the lungs and kidneys, which were made by lab technicians. The ribcage was delineated by a student. The delineations were made in Volumetool, which is delineation software written in the UMC Utrecht [19]. The delineations were made for the right and left sides separately in order to analyze them separately. The reported standard deviation was defined in equation 1 by Sonke *et al.* [20].

$$Stdev_{LR} = 0.36 \times Magnitude_{LR} \tag{1}$$

In equation 1, $Stdev$ is the standard deviation of the motion magnitude in that direction, in this case the left-right direction, hence the LR subscript. This equation holds for the anterior-posterior and cranial-caudal axes as well. The factor 0.36 is the standard deviation of a sin^6 function, which is used to model respiration as proposed by Lujan *et al.* [21]. The standard deviations of motion that were found were converted to a motion magnitude in that direction with equation 1. In the 2D representation in Figure 3, this motion magnitude of a single voxel would be the vertical distance between phases 0 and 6 for the vertical direction and the horizontal distance between phases 9 and 4 for the horizontal direction. A maximum and a mean motion magnitude for each direction was calculated

for each volume of interest. This was done for all patients and organs individually. To find a value that could be used as a motion magnitude for TBI patients, an average of all motion magnitudes of the surrogate population was calculated. The mean magnitude was used for all directions for the kidney. For the lungs, mean amplitudes were used in the left-right direction and in the anterior-posterior direction. The mean amplitude was not considered to be of much use in the superior-inferior direction, as motion in the upper part of the lungs is minimal. Therefore, for the inferior direction the maximum amplitude was used, the superior motion was assumed to be 0. The average of the mean amplitudes in the left-right and anterior-posterior directions of the lungs was compared to that of the ribcage to determine if there was a large difference in either direction.

C. Impact of intrafractional motion

The motion amplitudes described in the previous section were used to evaluate the effect of motion on organ dose in the VMAT-TBI treatment plans. Since these treatment plans were based on 3D-CT scans, the phase of the respiratory cycle was unknown for this CT scan. Therefore, the entire motion magnitude was used to expand and reduce volumes of interest to include the full range of motion from any point in the respiratory cycle. These expansions and reductions were done in Volumetool, which has a function to expand and reduce volumes non-uniformly with millimeter accuracy. An example of reductions and expansions is shown in Figure 4. The reduced and expanded volumes were manually polished when the generated volume seemed unrealistic. For example, an unpolished lung volume would be reduced or expanded around the pulmonary artery and the bronchi with the same motion magnitude as the diaphragm. The volume was adjusted to fit the original volume when such expansions were observed. The reduction represented a volume that would constantly cover a part of the organ with this motion magnitude, and the expansion represented a volume that represented the total range of motion of the organ. Dose volume histogram curves were used to evaluate the dose in the original, reduced, and expanded volumes.

D. Impact of interfractional motion

For this part of the study, an automated algorithm was used that was previously developed at the UMC Utrecht [22]. In this paper, the algorithm is applied to VMAT-TBI patients. TBI patients were treated in six fractions, and before each TBI fraction, a CBCT was taken. This CBCT was registered with the planning CT based on vertebrae using the deformable image registration algorithm EVolution [23]. The part of the planning CT that overlapped with the CBCT was deformed to match the CBCT anatomy and, therefore, adjust for changes in anatomy that had occurred between planning and treatment. Since the planning CT has a larger field of view than the CBCT, only a part was deformed. This deformed part was stitched back into the planning CT to create a synthetic CT. The delineations made on the planning CT were deformed to fit this synthetic CT. This synthetic CT was deformed in the

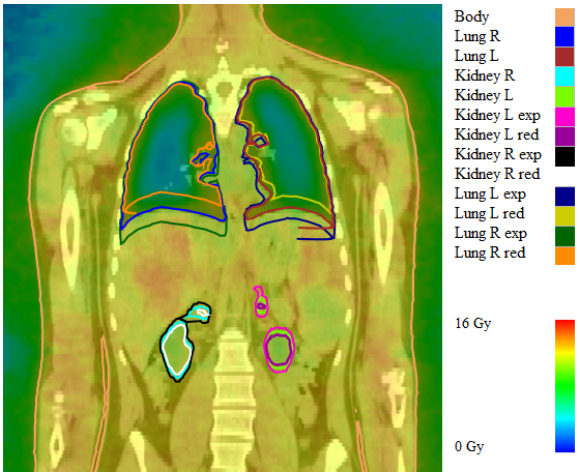

Fig. 4. This image shows the planning CT with expanded and reduced contours, overlapped with the dose distribution. The expansion and reduction of the volumes was done and dose was evaluated in these volumes. In the legend, the words left, right, expanded and reduced are abbreviated with L, R, exp and red, respectively

field of view of the CBCT to match the daily anatomy and had the electron density information that was measured on the planning CT. This electron density information is necessary to calculate the dose. Examples of these images are shown in Figure 5.

These deformed volumes were analyzed within the dose volume delivered in that fraction. The organ dose was evaluated by creating dose volume histograms of these deformed volumes; this was done in Volumetool. This fraction dose was compared with a dose constraint per fraction. Only organs in the CBCT field of view were evaluated. The analysis of organs outside of this field of view did not make sense, since the planning CT was not deformed in that area and all fractions would yield the same data. An example of this is shown in Figure 6. Therefore, all synthetic CT scans had to be visually inspected to determine if the OAR of interest was in the field of view. In addition, this inspection was performed to check if the synthetic CT reconstruction was successful.

III. Results

A. Intrafractional motion analysis

4D-CT data of 20 left kidneys, 21 right kidneys, and 31 pairs of lungs were used to calculate mid-position data. The different motion amplitudes were plotted in the figures listed in the Appendix A. Patients with dysfunctional lungs were excluded. This was done to evaluate respiratory motion in the most appropriate way. A dysfunctional lung may not induce respiratory motion on its side, and a functional lung on the other side may compensate and induce larger respiratory motion. The average motion amplitudes in the left-right and anterior-posterior directions were similar for the lungs and ribcages. The average motion amplitudes for each organ and direction are shown in Table II.

B. Intrafractional motion

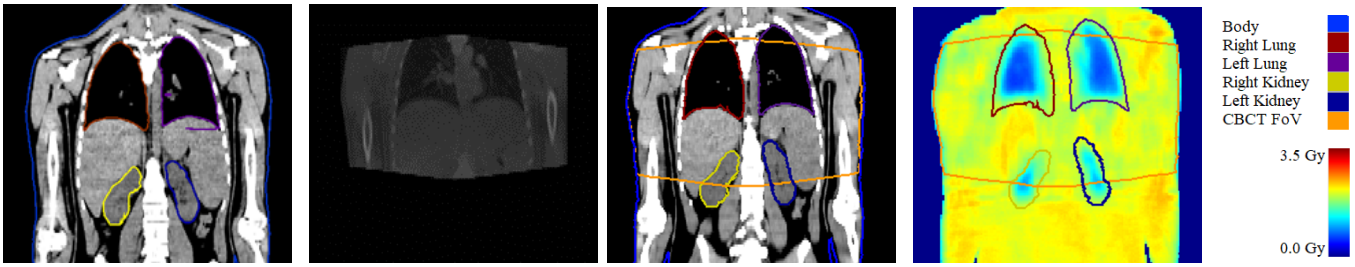

Fig. 5. Screen records from Volumetool to illustrate the method used for the interfraction study. The images show a planning CT with contours, a CBCT with the anatomy of that day, the synthetic CT that is used to make dose calculations on, and the calculated dose distribution.

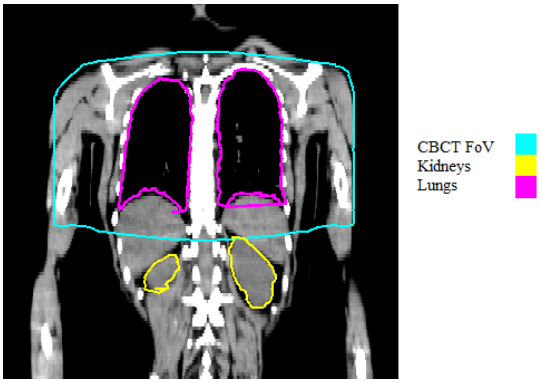

Fig. 6. In this example, the field of view of the CBCT is shown in cyan. The kidneys are outside the field of view, and therefore have to be excluded for analysis.

TABLE II
THE AVERAGE MOTION AMPLITUDES OVER ALL PATIENTS IN CENTIMETERS DERIVED FROM MID-POSITION DATA COMPUTED WITH 4D-CT DATA.

	Left	Right	Anterior	Posterior	Superior	Inferior
Left Kidney	0.06	0.06	0.1	0.1	0.3	0.3
Right Kidney	0.06	0.06	0.1	0.1	0.3	0.3
Left Lung	0.1	0.1	0.2	0.2	0	1.2
Right Lung	0.1	0.1	0.2	0.2	0	1.4

1) Kidneys: In the treatment plan of one patient the kidneys were not spared at all, therefore, this patient was excluded for the analysis of dosimetry in the kidneys. The average dose in the kidneys is shown in Figure 7, the contours are expanded and reduced with the found motion magnitude shown in Table II. The average and maximum differences found between the mean dose to the expanded and reduced kidney volumes compared to the mean dose to the original volume are listed in Table III. The dose in the original volumes exceeded the dose limit of 10 Gy in 5 of 26 cases for the left kidney and 9 of 26 cases for the right kidney. The dose in the expanded volumes exceeded the limit in 12 out of 26 cases for the left kidney and in 17 out of 26 cases for the right kidney. The amount of constraints that were exceeded is shown in Table V.

2) Lungs: The average dose in the lungs is shown in Figure 8, the contours are expanded and reduced with the found motion magnitude shown in Table II. In the past, the institute where these treatments were performed used a mean dose constraint of 10 Gy for the lungs. The average and maximum differences found between the mean dose in expanded and reduced lung volumes compared to the mean dose in the original volume are listed in Table IV. The dose in the original volumes exceeded the 8 Gy dose limit in 24 of 27 cases for the left lung and 12 of 27 cases for the right lung. The dose in the expanded volumes exceeded the limit in 25 cases for the left lung and in 23 out of 27 cases for the right lung. The dose in the original volumes exceeded the dose limit of 10 Gy in 1 of 27 cases for the left lung and none of 27 cases for the right lung. The dose to the expanded volumes exceeded the limit in 4 cases for the left lung and in 12 cases for the right lung. The amount of constraints that were exceeded is shown in Table V.

TABLE III
ABSOLUTE DIFFERENCE IN MEAN DOSE BETWEEN EXPANDED, REDUCED AND ORIGINAL VOLUME IN GRAY FOR THE LEFT AND THE RIGHT KIDNEY

Difference	Expansion Left	Reduction Left	Expansion Right	Reduction Right
Maximum	0.5 Gy	0.5 Gy	0.5 Gy	0.5 Gy
Average	0.3 Gy	0.3 Gy	0.3 Gy	0.3 Gy
Standard Deviation	0.1 Gy	0.1 Gy	0.1 Gy	0.1 Gy

TABLE IV
ABSOLUTE DIFFERENCE IN MEAN DOSE BETWEEN EXPANDED, REDUCED AND ORIGINAL VOLUME IN GRAY FOR THE LEFT AND THE RIGHT LUNG

Difference	Expansion Left	Reduction Left	Expansion Right	Reduction Right
Maximum	0.7 Gy	0.7 Gy	1.0 Gy	0.8 Gy
Average	0.6 Gy	0.5 Gy	0.8 Gy	0.6 Gy
Standard Deviation	0.1 Gy	0.1 Gy	0.1 Gy	0.1 Gy

TABLE V
THE AMOUNT OF TIMES THAT THE DOSE CONSTRAINT WAS EXCEEDED FOR EACH ORGAN AS A SHARE OF TOTAL PATIENT POPULATION PER ORGAN.

Organ (dose constraint)	Expanded	Original
Left kidney (10 Gy)	10/26	5/26
Right kidney (10 Gy)	12/26	9/26
Left lung (10 Gy)	4/27	1/27
Right lung (10 Gy)	0/27	0/27
Left lung (8 Gy)	25/27	24/27
Right lung (8 Gy)	23/27	12/27

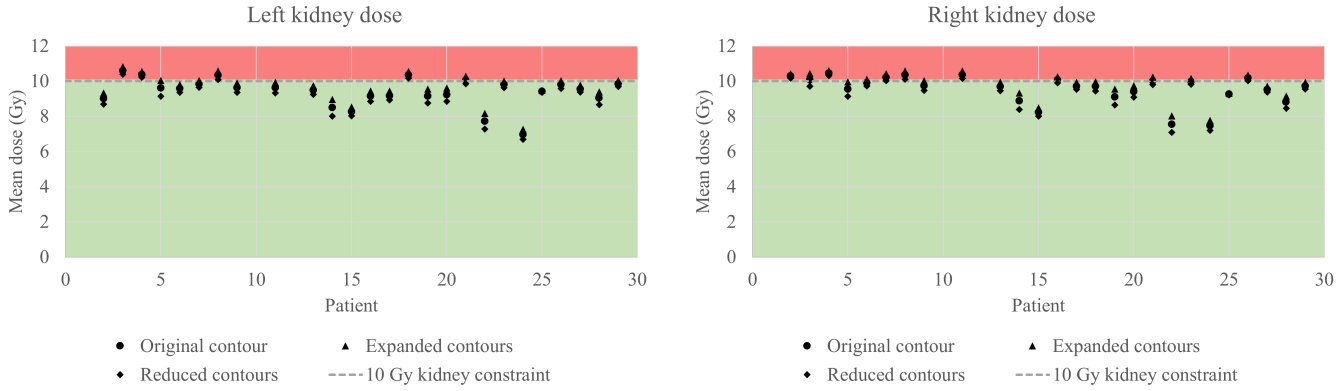

Fig. 7. Mean dose calculated for the original, the expanded and the reduced volumes of the kidneys for the VMAT-TBI patients. The dashed line indicates the dose constraint for the kidneys.

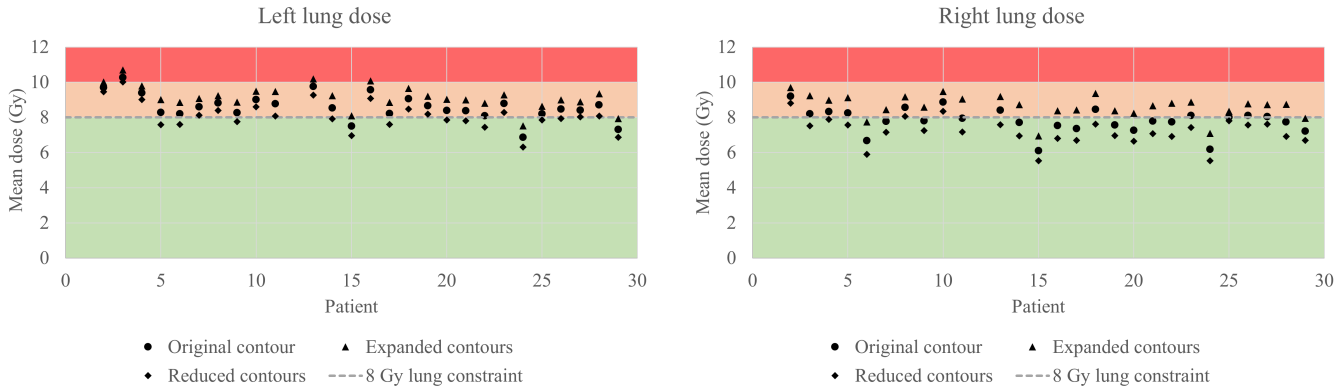

Fig. 8. Mean dose calculated for the original, the expanded and the reduced volumes of the lungs for the VMAT-TBI patients. The dashed line indicates the dose constraint for the lungs. The red area indicates a mean dose exceeding the 10 Gy mean dose constraint, and the orange area indicates a mean dose exceeding the 8 Gy mean dose constraint.

TABLE VI
KIDNEY DOSE DIFFERENCE BETWEEN FRACTION WITH LOWEST MEAN DOSE AND FRACTION WITH HIGHEST MEAN DOSE.

Difference in mean dose	Left kidney	Right kidney
Maximum	0.13 Gy	0.12 Gy
Average	0.04 Gy	0.04 Gy
Standard Deviation	0.03 Gy	0.03 Gy

TABLE VII
LUNG DOSE DIFFERENCE BETWEEN FRACTION WITH LOWEST MEAN DOSE AND FRACTION WITH HIGHEST MEAN DOSE.

Difference in mean dose	Left lung	Right lung
Maximum	0.08 Gy	0.1 Gy
Average	0.04 Gy	0.04 Gy
Standard Deviation	0.02 Gy	0.02 Gy

C. Interfractional motion

Two patients received a new treatment plan between fractions. One patient was treated in a fraction where the correction of the CBCT was not performed correctly. This resulted in a failed reconstruction of the synthetic CT and, consequently, in the dose calculation and contour propagation.

1) Kidneys: Patients were excluded for this analysis when the kidneys were not within the CBCT field of view, the number of patients and fractions for each organ is listed in Table VI. Outside of the CBCT field of view, the synthetic CT was the same as the planning CT, and the used model would compare the planned dose to itself six times. This would result in an underestimation of the average effect of interfractional motion on the mean dose. As in the intrafractional study, one patient was excluded for kidney analysis because the kidneys were not spared in the treatment plan. Patients were excluded for this analysis when the kidneys were outside of the field of view of the CBCT. The mean dose in the kidneys for each fraction and patient is shown in Figure 9. For each patient, the dose difference between the fraction with the lowest mean dose and the fraction with the highest mean dose was determined. For each organ, an average of this difference was recorded in Table VI with the sample standard deviation. In addition, the maximum of these differences in all patients was recorded in Table VI.

2) Lungs: In many CBCTs, a small cranial part of the lung was outside of the field of view of the CBCT. Since motion in the cranial end of the lung is generally minimal, its absence in the CBCT was not considered relevant for the analysis of dose variation. The mean dose in the lungs for each fraction and patient is shown in Figure 10. For each patient, the dose

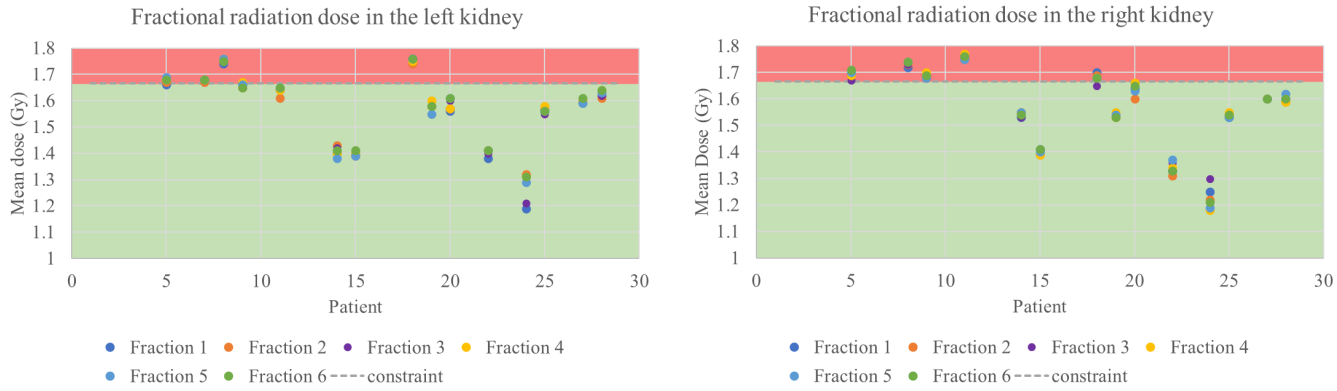

Fig. 9. The mean dose in the kidneys for each fraction for all patients. The red area indicates a dose exceeding the constraint for each fraction. The vertical axis is zoomed in to visualize the differences between the fractions better.

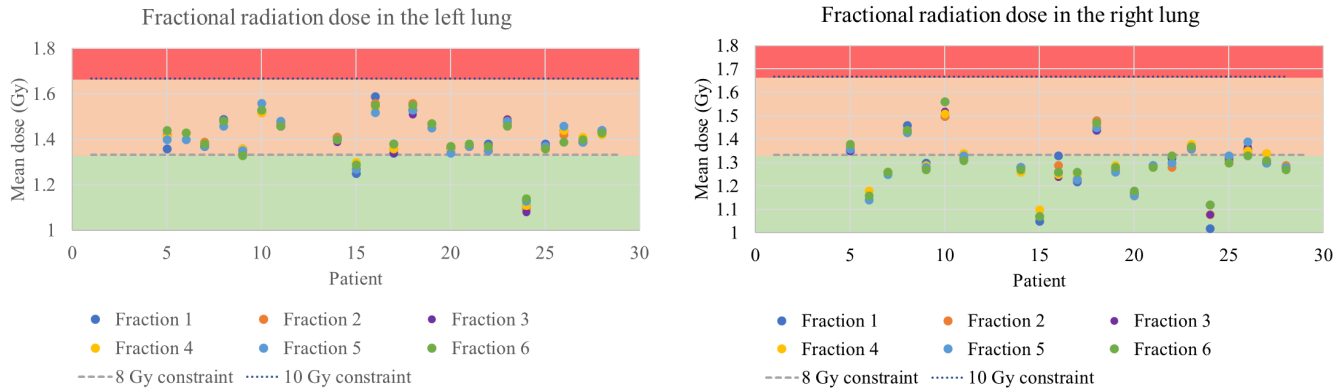

Fig. 10. The mean dose in the lungs for each fraction for all patients. The red area indicates a dose exceeding the constraint for a mean dose of 10 Gy, the orange part indicates a dose exceeding the constraint for a mean dose of 8 Gy. The vertical axis is zoomed in to visualize the differences between the fractions better.

difference between the fraction with the lowest mean dose and the fraction with the highest mean dose was determined. For each organ, an average of this difference was recorded in Table VII with the sample standard deviation. In addition, the maximum dose difference that was found in all patients that were irradiated in six fractions was listed. Therefore, this fraction was excluded. One patient was treated with two different plans. The first three fractions were treated with a different plan than the last three, but the CBCTs of the first plan seem to have been incorrectly registered. These three fractions were excluded. This was only a problem for lung analysis as the kidneys were outside of the CBCT field of view for this patient.

IV. Discussion

In this cohort of TBI patients treated with VMAT in the UMC Utrecht, the dosimetric impact of intrafractional and interfractional motion was assessed for the kidneys and lungs for treatment delivered by VMAT. This cohort size is similar to the literature in similar studies [5, 10, 24].This impact was studied to investigate whether a 4D-CT or a PRV was necessary for the treatment planning of these patients to ensure a robust dose distribution against intra- and interfraction variations. A typical intrafractional motion magnitude was determined after a motion study in a surrogate population. On average, an expansion with this typical magnitude of respiratory motion results in a 0.3 ± 0.1 Gy higher mean dose in the kidneys. This expansion results in a 0.6 ± 0.1 Gy higher mean dose in the left lung and a 0.8 ± 0.1 Gy higher dose in the right lung. In the UMC Utrecht, VMAT-TBI patients are treated in 6 fractions, and the mean dose difference between these fractions was studied. The largest difference between different fractions of the same treatment in mean dose is 0.04 $\pm$ 0.02 Gy on average for the lungs and 0.04 $\pm$ 0.03 Gy for the kidneys. To the author's knowledge, this study is the first to investigate this effect for VMAT-TBI with real patient plans.

The study on intrafractional motion was conducted with a volume that is expanded and reduced with the motion magnitude of the entire organ motion in all directions, from minimum to maximum. When the dose is calculated in these volumes, it must be taken into account that this method has a systematic error. Expansion with the entire motion magnitude is an overestimation of the motion when the 3D planning CT is not taken at the maximum in- or exhale phase. In addition, dosimetric analysis in an expanded or reduced volume does not consider the respiratory cycle. An organ will not remain in one of the phases but will continuously change position throughout the respiratory cycle. In reality, the dose difference is smaller

than the values reported in this study.

In this study, the mean dose in the lungs was calculated for all of the lung volume. However, the lung dose is often evaluated in a lung volume that is uniformly reduced by 5 mm in the clinic to avoid underdosage of the ribs [25]. The results of this study suggest that the lung dose is barely below the 8 Gy constraint in VMAT-TBI for the original contours. The mean lung dose is expected to be less than 8 Gy when looking at the original lung volumes uniformly reduced by 5 mm. This 5 mm reduction was performed on the lung volumes of one patient. For this patient, the average mean dose difference for the expanded, reduced, and original contours for both lungs is 1.1 Gy. This would mean that the constraints may not be exceeded as often as the Table V suggests.

For both the intra- and the interfractional study, the dosimetric impact of lung motion differed for the left and right sides. This is likely due to the heart that sticks out in the left lung, which is part of the target volume. Recently, in the UMC Utrecht, the decision was made to apply a mean dose constraint of 8 Gy to the heart as well. This is expected to decrease the difference in dosimetric impact between the left and right lung.

The risk of lung toxicity can be reduced by reducing the biologically effective dose (BED), for example, by lowering the total dose, lowering dose rates, or fractionation [9]. No literature was found that defined a dose response relationship for lung toxicities after radiotherapy with the same dose rate and fractionation as VMAT-TBI in the UMC Utrecht. Therefore, a physician had to be consulted to understand the clinical relevance of the dose differences found in this study.

The impact of intrafractional motion on the mean dose to the lungs and kidneys can be considered acceptable. It is not necessary to take 4D-CT scans of patients for treatment planning. With the comments previously discussed on the intrafractional method in mind, it can be concluded that on average the dosimetric impact on mean kidney dose will be less than 0.3 Gy. In addition, the average impact on the mean lung dose will be less than 0.6 Gy for the left lung and 0.8 Gy for the right lung.

The dose differences found in this group of patients are small. The clinical relevance was discussed with a physician and it was concluded that differences such as these are not clinically relevant. The impact of interfractional motion on the mean dose to the lungs and kidneys can be considered acceptable. VMAT-TBI plans are robust enough and do not require daily replanning or a PRV. When the fractions of therapy are compared, the differences in mean dose are small. When the fraction with the lowest mean dose and the fraction with the highest mean dose are compared, the average difference in mean dose is 0.04 Gy for all organs on both sides. If that difference occurred as an exceedance of the planned dose for each fraction, the total impact would be 0.24 Gy.

Acknowledgment

The author would like to thank Enrica Seravalli and Bianca Hoeben for the supervision of this project, as well as Peter Stijnman for helping with the algorithm used in the interfractional study that enabled dose evaluation on daily CBCT anatomy. In addition, the author would like to thank Marlies Goorden for supervision from Delft University of Technology.

References

[1] Joep C Stroom and Ben JM Heijmen. “Limitations of the planning organ at risk volume (PRV) concept”. In: *International Journal of Radiation Oncology* Biology* Physics* 66.1 (2006), pp. 279–286.

[2] Toshihiro Sera. “Computed tomography”. In: *Transparency in Biology: Making the Invisible Visible* (2021), pp. 167–187.

[3] Adam Hutchinson and Pete Bridge. “4DCT radiotherapy for NSCLC: a review of planning methods”. In: *Journal of Radiotherapy in Practice* 14.1 (2015), pp. 70–79.

[4] Stephen J. Gardner, Joshua Kim, and Indrin J. Chetty. “Modern Radiation Therapy Planning and Delivery”. In: *Hematology/Oncology Clinics of North America* 33.6 (2019). Contemporary Topics in Radiation Medicine, Part I: Current Issues and Techniques, pp. 947–962. ISSN: 0889-8588. DOI: https://doi.org/10.1016/j.hoc.2019.08.005. URL: https://www.sciencedirect.com/science/article/pii/S088985881930098X.

[5] Bora Tas et al. “Total-body irradiation using linac-based volumetric modulated arc therapy: Its clinical accuracy, feasibility and reliability”. In: *Radiotherapy and Oncology* 129.3 (2018), pp. 527–533.

[6] Ayse Gulbin Kavak et al. “Impact of respiratory motion on lung dose during total marrow irradiation”. In: *Frontiers in Oncology* 12 (2022), p. 924961.

[7] SA Carruthers and MM Wallington. “Total body irradiation and pneumonitis risk: a review of outcomes”. In: *British journal of cancer* 90.11 (2004), pp. 2080–2084.

[8] Raymond Miralbell et al. “Renal toxicity after allogeneic bone marrow transplantation: the combined effects of total-body irradiation and graft-versus-host disease.” In: *Journal of clinical oncology* 14.2 (1996), pp. 579–585.

[9] Bianca AW Hoeben et al. “ESTRO ACROP and SIOPE recommendations for myeloablative Total Body Irradiation in children”. In: *Radiotherapy and Oncology* 173 (2022), pp. 119–133.

[10] Enrica Seravalli et al. “Treatment robustness of total body irradiation with volumetric modulated arc therapy”. In: *Physics and Imaging in Radiation Oncology* 29 (2024), p. 100537.

[11] E Hoseinnezhad Zarghani, G Geraily, and T Hadisinia. “Comparison of different TBI techniques in terms of dose homogeneity–review study”. In: *Cancer/Radiothérapie* 25.4 (2021), pp. 380–389.

[12] Bianca AW Hoeben et al. “Total body irradiation in haematopoietic stem cell transplantation for paediatric acute lymphoblastic leukaemia: review of the literature and future directions”. In: *Frontiers in Pediatrics* 9 (2021), p. 774348.

[13] Susanta K Hui et al. “CT-based analysis of dose homogeneity in total body irradiation using lateral beam”. In: *Journal of applied clinical medical physics* 5.4 (2004), pp. 71–79.

[14] J Dyk. “The physical aspects of total and half body photon irradiation.” In: *AAPM report* 17 (1986), pp. 22–24.

[15] K Dj. “An Overview of Image-Guided Radiotherapy (IGRT)”. In: *OMICS Journal of Radiology* 3.4 (2014), pp. 2–4.

[16] Karl Otto. “Volumetric modulated arc therapy: IMRT in a single gantry arc”. In: *Medical physics* 35.1 (2008), pp. 310–317.

[17] Lawrence Lechuga and Georg A Weidlich. “Cone beam CT vs. fan beam CT: a comparison of image quality and dose delivered between two differing CT imaging modalities”. In: *Cureus* 8.9 (2016).

[18] J. W. H. Wolthaus et al. “Reconstruction of a time-averaged midposition CT scan for radiotherapy planning of lung cancer patients using deformable registration”. In: *Medical Physics* 35.9 (2008), pp. 3998–4011. DOI: https://doi.org/10.1118/1.2966347. eprint: https://aapm.onlinelibrary.wiley.com/doi/pdf/10.1118/1.2966347. URL: https://aapm.onlinelibrary.wiley.com/doi/abs/10.1118/1.2966347.

[19] Gijsbert H Bol et al. “Simultaneous multi-modality ROI delineation in clinical practice”. In: *Computer methods and programs in biomedicine* 96.2 (2009), pp. 133–140.

[20] Jan-Jakob Sonke et al. “Frameless stereotactic body radiotherapy for lung cancer using four-dimensional cone beam CT guidance”. In: *International Journal of Radiation Oncology* Biology* Physics* 74.2 (2009), pp. 567–574.

[21] Anthony E Lujan et al. “A method for incorporating organ motion due to breathing into 3D dose calculations”. In: *Medical physics* 26.5 (1999), pp. 715–720.

[22] Maureen Groot Koerkamp et al. “Automated dose evaluation on daily cone-beam computed tomography for breast cancer patients”. In: *Radiotherapy and Oncology* 200 (2024), p. 110541.

[23] B Denis de Senneville et al. “EVolution: an edge-based variational method for non-rigid multi-modal image registration”. In: *Physics in Medicine & Biology* 61.20 (2016), p. 7377.

[24] Filipa Guerreiro et al. “Intra-and inter-fraction uncertainties during IGRT for Wilms’ tumor”. In: *Acta Oncologica* 57.7 (2018), pp. 941–949.

[25] Chunhui Han, Timothy E Schultheisss, and Jeffrey YC Wong. “Dosimetric study of volumetric modulated arc therapy fields for total marrow irradiation”. In: *Radiotherapy and Oncology* 102.2 (2012), pp. 315–320.

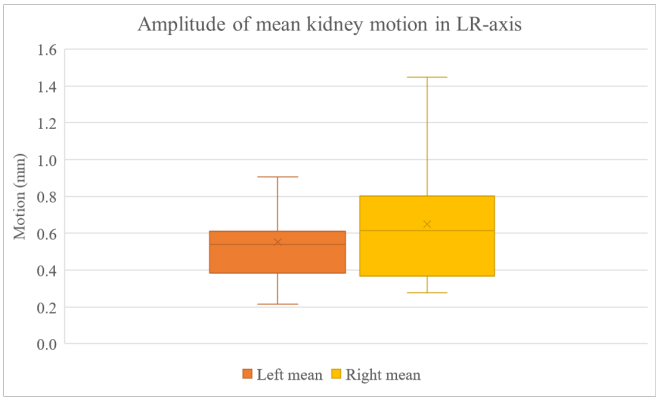

Fig. 11. Motion in the left-right direction of the kidneys.

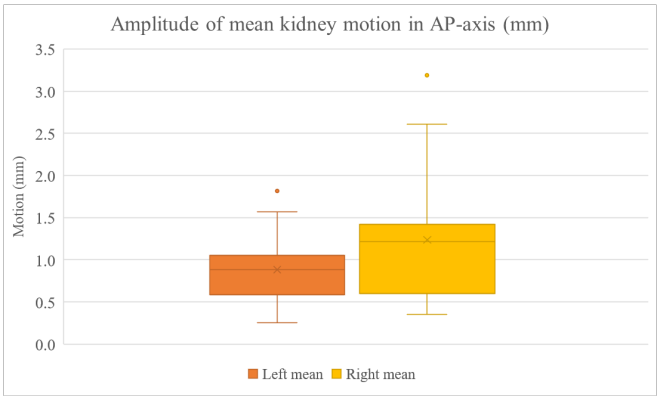

Fig. 12. Motion in the anterior-posterior direction of the kidneys.

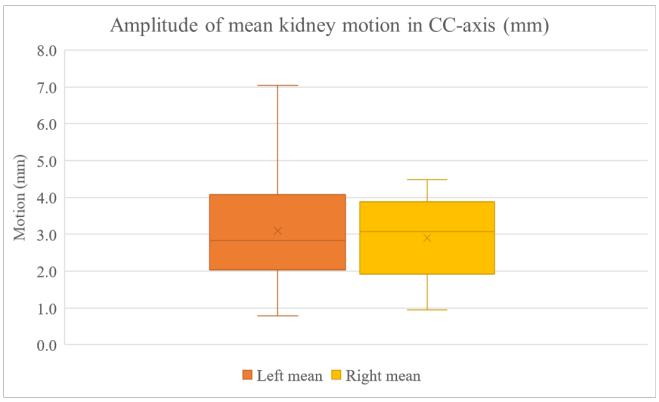

Fig. 13. Motion in the superior-inferior direction of the kidneys.

APPENDIX

This appendix contains box-and-whisker plots that show the motion magnitudes that were analyzed from the surrogate patient population. The kidney movement is shown in the figures 11 12 and 13, the lung movement is shown in the figures 14, 15 and 16.

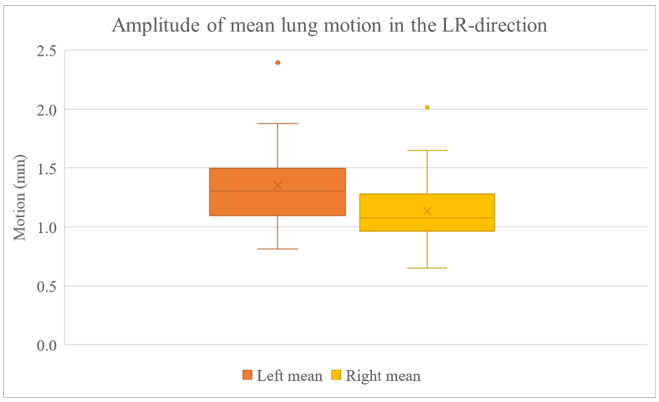

Fig. 14. Motion in the left-right direction of the lungs.

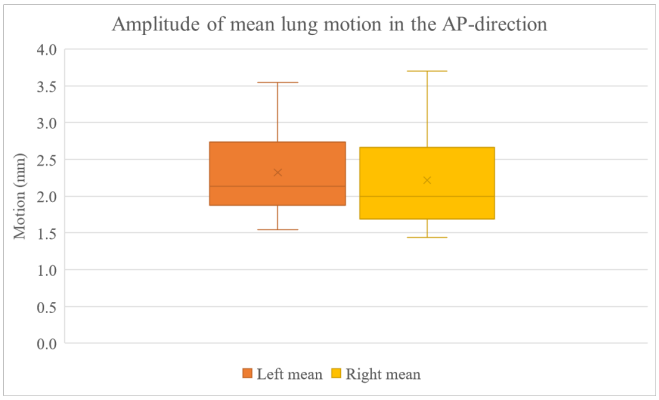

Fig. 15. Motion in the anterior-posterior direction of the lungs.

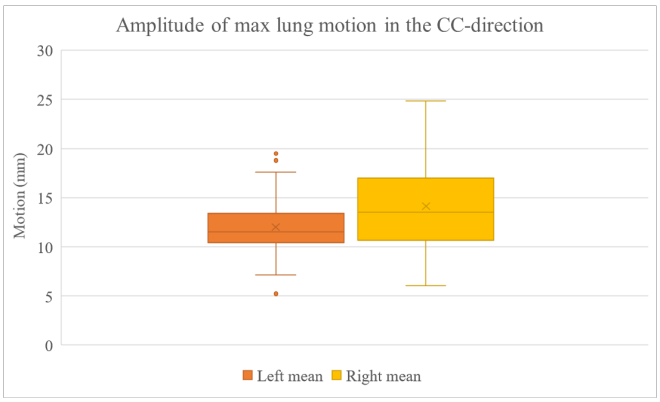

Fig. 16. Motion in the superior-inferior direction of the lungs.